

1 **Human amplification of drought-induced biomass burning in Indonesia since 1960**

2  
3 **R. D. Field<sup>1</sup>, G. R. van der Werf<sup>2</sup>, S.S.P. Shen<sup>3</sup>**

4 *1. Department of Physics, University of Toronto, Toronto, Canada*

5 *2. Faculty of Earth and Life Sciences, VU University Amsterdam, Amsterdam,*  
6 *Netherlands*

7 *3. Department of Mathematics and Statistics, San Diego State University, San Diego,*  
8 *United States*

9  
10 **Biomass burning in Indonesia is a singularly large source of greenhouse gas**  
11 **emissions globally <sup>1,2</sup>, with pronounced regional impacts on air quality <sup>3,4</sup>. Analysis**  
12 **of satellite observations since 1997 has shown that these fires burn predominantly**  
13 **during drought periods <sup>5</sup>, but this relatively short record limits our ability to**  
14 **understand the underlying climatic and anthropogenic causes of the fires. Here, we**  
15 **provide a continuous monthly record of severe fires in Indonesia from 1960 to 2006**  
16 **using the visibility reported at airports, which was found to be an excellent proxy**  
17 **for particulate matter emissions. This proxy indicated that air quality during the**  
18 **haze events in Indonesia was worse, by a factor of five, than extreme periods in**  
19 **cities with the world's worst air quality. This dataset also indicated that large fire**  
20 **events have occurred in Sumatra at least since the 1960s, but in Kalimantan only**  
21 **since the 1980s, despite the occurrence of several severe droughts during 1960-1980.**  
22 **This difference can be attributed to different patterns of intensified land use and**  
23 **population growth. Between the droughts of 1972 and 1982, Kalimantan changed**  
24 **from being highly fire resistant to fire prone due to accelerated deforestation and**  
25 **transmigration. This period thus marks the point when one of the world's great**  
26 **tropical forests became one of the world's largest sources of pollution. In the**  
27 **presence of intensive land use, furthermore, there is a non-linear relationship**  
28 **between rainfall and fire, whereby fire events occur only during years when rainfall**  
29 **falls below a certain threshold. Finally, we find that while fires in Indonesia have**  
30 **become synonymous with El Niño <sup>1,6,7,8,9,10</sup>, the Indian Ocean Dipole is in fact as**  
31 **important a contributing factor. Improved understanding of these controls may**  
32 **help to better assess future fire risk in Indonesia with changing climate <sup>11</sup> and land**  
33 **use <sup>12,13</sup>.**  
34

1 During 1997-2006, there were two major fire episodes in Indonesia (1997/98, 2006) and  
2 two minor episodes (2002, 2004) detected in the Global Fire Emissions Database (GFED)  
3<sup>14</sup>, which occurred during droughts of different strengths<sup>5,9,10</sup>. Prior to this, there are no  
4 high-quality, continuous records of the fires. There are, however, case-by-case accounts  
5 of coincident drought and fire years during the 1980s and early 1990s<sup>15</sup>, also detected in  
6 elevated ozone and aerosol concentrations from the Total Ozone Mapping Spectrometer  
7<sup>3,6</sup>.

8  
9 The Indonesian fires are unique in terms of the continuous burning of dense peat soils for  
10 up to four consecutive months<sup>1</sup>, which produce aerosol concentrations high enough to  
11 significantly reduce visibility<sup>8,16,17</sup>. In order to better understand the severity of biomass  
12 burning haze and its underlying causes, we used visibility records from Sumatra and  
13 Kalimantan's World Meteorological Organization (WMO) level meteorological stations  
14 to calculate monthly mean extinction coefficient ( $B_{ext}$ ) since 1960 ( Figures 1-3). Three  
15 stations in each of Sumatra and Kalimantan had data back to 1960.

16  
17 We found an excellent correspondence between regional  $B_{ext}$  and total particulate matter  
18 (TPM) estimates from the GFED for both Sumatra ( $R^2 = 91\%$ ) and Kalimantan ( $R^2 =$   
19  $85\%$ ) for the period of 1997-2006. As an indication of the severity of the 1997 haze event  
20 and its impact on air quality, the extreme monthly  $B_{ext}$  values from other stations near the  
21 centre of the main burning regions (maximum  $16.6 \text{ km}^{-1}$ ) were over five times greater  
22 than the extreme monthly  $B_{ext}$  values at the cities recognized as having the world's worst  
23 air quality (maximum  $3.1 \text{ km}^{-1}$ ) (Table S1).

24  
25 In Sumatra, the extended  $B_{ext}$  signal captured the events in 1982, 1987, 1991 and 1994  
26 (Figure 2b)<sup>8</sup>. There were also large, previously unidentified events in 1961, 1963 and  
27 1972 of a slightly lesser magnitude than those in the 1990s, but easily distinguishable  
28 from the background  $B_{ext}$  level. All events from 1960 to 2006 occurred during periods of  
29 anomalously low seasonal rainfall (Figure 2c). Conversely, there was an absence of  
30 severe events during non-drought years, despite regular reductions in dry-season rainfall.

31  
32 We estimated this non-linear relationship between precipitation and haze using piecewise  
33 linear regression, splitting the data into an early period (1960-1983) and recent period  
34 (1984-2006) to detect any possible changes in the sensitivity of fire to drought (see  
35 Methods). During 1960-1983, 5-month back-totalled precipitation was the best predictor  
36 variable, explaining 67% of the variance in  $B_{ext}$  over Sumatra, with a threshold of 609  
37 mm (Table 1, Figure 2). Below this threshold, there was a sensitivity of  $-0.011 \text{ km}^{-1}\text{mm}^{-1}$ ,  
38 indicating an increase in  $B_{ext}$  with decreasing precipitation. During the 1984-2006 period,  
39 5-month precipitation could explain 85% of the variance in  $B_{ext}$ , with a threshold of  
40 631mm and a below-threshold sensitivity of  $-0.015 \text{ km}^{-1}\text{mm}^{-1}$ . The improved  
41 predictability during the 1984-2006 period can be attributed in part to the superior-  
42 quality-precipitation data during that period, and perhaps to a slightly stronger sensitivity  
43 of the Sumatran fire environment to drought.

44  
45 In Kalimantan, there was a much different history of biomass burning. Severe haze  
46 events under drought conditions are evident from 1982 onwards, but unlike Sumatra, are

1 absent during the 1960s and 1970s (Figure 3b). Atmospheric trajectory analysis showed  
2 that the absence of haze during this period was not attributable to differences in wind  
3 flow. The 1972 and 1997 droughts, for example, had similar patterns of atmospheric  
4 transport between the burning region and the visibility stations, but severe haze was  
5 observed only in 1997 (see Supplementary Material).

6  
7 More quantitatively, the 4-month precipitation was the best predictor during 1984-2006  
8 over Kalimantan, explaining 78% of the variance in  $B_{ext}$ , with a precipitation threshold of  
9 672mm and a below-threshold sensitivity of  $-0.007 \text{ km}^{-1}\text{mm}^{-1}$  (Table 1, Figure 3). In  
10 contrast, such a relationship was absent from 1960-1983, with only 13% of the variance  
11 in  $B_{ext}$  explained by the 4-month precipitation, and a below-threshold sensitivity of  $-0.001$   
12  $\text{km}^{-1}\text{mm}^{-1}$ , which was not statistically distinguishable from zero. Whereas in Sumatra  
13 there was only a small increase in fire sensitivity to drought, the Kalimantan fire  
14 environment changed from highly fire-resistant to highly fire-prone at some point  
15 between the droughts of 1972 and 1982.

16  
17 Drought acts as the trigger for fire occurrence, but it is humans who ignite the fires. How  
18 do we explain the difference in the evolution of the fire environments in Sumatra and  
19 Kalimantan since the 1960s?

20  
21 In Indonesia, fire is used primarily to clear vegetation waste, and is closely associated  
22 with deforestation and agricultural expansion. The number of ignitions depends on the  
23 extent of these activities, which also tend to lower the resilience of tropical forests to  
24 drought through changes in moisture balance<sup>7,18</sup>. Indonesia's overall deforestation rate  
25 from 1950 to 1997 was 1.1%, but from 1950-1985, the deforestation rate in Kalimantan  
26 (0.7%) was half that of Sumatra (1.4%). It was only during 1985 to 1997 that the  
27 deforestation rate in Kalimantan (2.2%) began to approach that of Sumatra (2.6%) (See  
28 Supplementary Materials).

29  
30 Kalimantan's later deforestation is characteristic of broader development patterns,  
31 reflected by trends in population and agriculture. Sumatra had population growth rates  
32 3.8 times greater than Kalimantan during the first half of the 20<sup>th</sup> century (Figure S12).  
33 During the 1960s and 1970s, population growth in Sumatra accelerated rapidly to over 8  
34 inhabitants decade<sup>-1</sup> km<sup>-2</sup>, but lagged behind in Kalimantan, approaching Sumatra's  
35 1960s growth rates only in the 1980s. This difference in population growth between the  
36 two regions was in part due to the Indonesian government's policy of transmigration to  
37 ease population pressure on Java and, later, to develop Indonesia's remote forested  
38 regions. Sumatra was the main target region of transmigration through the 1960s and  
39 1970s, while Kalimantan became a significant target region in the 1980s. In Kalimantan,  
40 the effects of this population shift on land-cover change were exacerbated by a change in  
41 focus from small-scale subsistence agriculture to large-scale industrial agriculture and  
42 agro-forestry, which have larger land-use footprints. Peatlands drained under the Mega  
43 Rice Project of the 1990s, for example, were the single biggest contributor to emissions  
44 across all of Indonesia during the 1997 fire event (See Supplementary Materials).

45

1 Overall, we attribute the difference in evolution of Sumatra's and Kalimantan's fire  
2 environments to different patterns of human activity and government policy. Much of  
3 Kalimantan remained relatively undeveloped until the 1980s, which explains the prior  
4 absence of fire seen in the  $B_{ext}$  record, despite several severe droughts in the 1960s and  
5 1970s.

6  
7 In addition to their different fire environments, drought over Sumatra and Kalimantan is  
8 influenced by different patterns of zonal circulation in the tropics. Whereas haze events  
9 have been attributed predominantly to El Niño conditions<sup>8</sup>, there is strong evidence that  
10 the Indian Ocean Dipole (IOD) also contributes to drought over Indonesia<sup>19,20,21</sup>. We  
11 found that over Sumatra, the Niño 3.4 sea-surface temperature (SST) index could explain  
12 30% of the variability in mean July-November precipitation under a linear model,  
13 compared to 61% explained by the Dipole Mode Index (DMI) (Figure S2). Over  
14 Kalimantan, the Niño 3.4 could explain 58% of the variability in precipitation, compared  
15 to 49% explained by the DMI, but a combined index could explain 72% of the variability.

16  
17 It is therefore important that SST anomalies over both the Pacific and Indian Oceans be  
18 monitored in preventing and mitigating future fire events. While the 1994 and 2006  
19 events, for example, did occur during moderate El Niño conditions<sup>9,10</sup>, it was the positive  
20 IOD conditions which distinguished them from 2002, when the drought and haze were  
21 weaker. The 1961 event occurred under neutral ENSO and positive IOD conditions, but  
22 conversely, the 1982 drought occurred under strong El Niño conditions and neutral IOD  
23 conditions. The severity of the 1997 event appears attributable to the combined strength  
24 of the El Niño and the IOD.

25  
26 With the presence of intensive land-use, severe fire years have occurred when seasonal  
27 rainfall was below a given threshold, owing to either or both El Niño or Indian Ocean  
28 Dipole conditions. This is distinct from other regions in the tropics with large fire  
29 emissions, such as Brazil and the Congo basin, which have consistent burning each dry  
30 season due to less interannual variability in the length and intensity of the dry season<sup>14</sup>.  
31 Our precipitation threshold estimates can therefore serve as benchmarks to identify  
32 periods of severe haze risk, aiding in the interpretation of seasonal rainfall outlooks<sup>22</sup> for  
33 operational fire management.

34  
35 Such mitigation measures are particularly important under a changing climate, given the  
36 possibility of more persistent El Niño-like conditions<sup>23</sup>, reduced rainfall over Indonesia's  
37 main burning regions<sup>11</sup>, and a positive feedback between reduced soil moisture and  
38 reduced precipitation in Indonesia<sup>24</sup>. There is also little evidence that deforestation rates  
39 in Indonesia, and hence the use of fire, will decline in the near future. Among countries  
40 with humid tropical forests, Indonesia's current deforestation rate of 3.4% per year is  
41 second only to Brazil<sup>13</sup>. There is also a projected increase in the extent of large-scale oil  
42 palm plantations<sup>25</sup>, partly to meet growing demand for biofuels<sup>12</sup>. Since droughts are  
43 inevitable, and may become more severe, Indonesia's future fire regime depends strongly  
44 on the extent of these types of human activity.

45

1 **Methods summary**

2 For each region, we considered back-totalled rainfall of up to five-months as predictor  
3 variables. More sophisticated drought indices were not considered, having been shown  
4 for 1997-2006 to not provide any advantage over simple rainfall totals<sup>5</sup>. We used the best  
5 available precipitation data for each of the 1960-1983 and 1984-2006 analysis periods.  
6 The NCEP Precipitation over Land (PRECL) dataset<sup>26</sup> beginning in 1948 was used for  
7 the 1960-1983 period, but was found to have a much more sparse gauge observation  
8 network from the 1980s onwards (Figure S1). For the 1984-2006 period, we therefore  
9 used data from the Global Precipitation Climatology Project (GPCP),<sup>27</sup> which  
10 incorporates infrared and microwave satellite retrievals and rain gauge observations,  
11 covering 1979-present.

12

13 We used piecewise regression to estimate the non-linear relationship between drought  
14 and  $B_{ext}$ <sup>5</sup>. This technique provided an explicit estimate of drought threshold, and of the  
15 sensitivity of  $B_{ext}$  to changes in precipitation below this threshold. Physically, the use of a  
16 threshold-based model corresponds to moisture ignition thresholds of fuels, particularly  
17 in drained peatland<sup>5,28</sup>. The model consists of two linear segments, constrained to be  
18 equal at an unknown threshold  $\alpha$ , and is given by

19 
$$B_{ext} = \begin{cases} \beta_0 + \beta_1 x & , \quad x \leq \alpha \\ \beta_0 + \beta_1 x + \beta_2 (x - \alpha) & , \quad x > \alpha \end{cases}$$

20 where  $\beta_1$  is the slope of the line below  $\alpha$ ,  $\beta_1 + \beta_2$  is the slope of the line above  $\alpha$ , and  $x$   
21 is a given predictor variable, for example, 3-month back-totalled precipitation. The  
22 below-threshold slope  $\beta_1$  quantifies the degree to which  $B_{ext}$  varies with precipitation.

23 Across the different back-totalling periods, we assessed goodness of fit using the  
24 coefficient of determination  $R^2$ , and provide 95% confidence intervals for all estimated  
25 parameters using fully-paired bootstrapping with 2000 re-samples<sup>29</sup>. Scatter plot versions  
26 of Figures 2 and 3 are shown in Figures S7 and S8, which emphasize the structure of the  
27 piecewise model.

28

1 **Acknowledgements**

2 We thank Will Spangler at the National Center for Atmospheric Research for assistance  
3 in processing the visibility data, and Norah MacKendrick for editorial assistance. RF was  
4 supported by an NSERC PGS-D scholarship.

## 1 **References**

- 2 1. Page, S.E. *et al.* The amount of carbon released from peat and forest fires in  
3 Indonesia during 1997. *Nature* **420**, 61-65 (2002).
- 4 2. van der Werf, G.R. *et al.* Interannual variability in global biomass burning  
5 emissions From 1997 to 2004. *Atmospheric Chemistry and Physics* **6**, 3423-3441  
6 (2006).
- 7 3. Thompson, A.M. *et al.* Tropical tropospheric ozone and biomass burning. *Science*  
8 **291**, 2128-2132 (2001).
- 9 4. Kunii, O. *et al.* The 1997 haze disaster in Indonesia: its air quality and health  
10 effects. *Archives of Environmental Health* **57**, 16-22 (2002).
- 11 5. Field, R.D. and Shen, S.S.P. Predictability of carbon emissions from biomass  
12 burning in Indonesia from 1997 to 2006. *Journal of Geophysical Research -*  
13 *Biogeosciences* (2008).
- 14 6. Kita, K., Fujiwara, M., and Kawakami, S. Total ozone increase associated with  
15 forest fires over the Indonesian region and its relation to the El Niño-Southern  
16 oscillation. *Atmospheric Environment* **34**, 2681-2690 (2000).
- 17 7. Siegert, F., Ruecker, G., Hinrichs, A., and Hoffmann, A.A. Increased damage from  
18 fires in logged forests during droughts caused by El Niño. *Nature* **414**, 437-440  
19 (2001).
- 20 8. Wang, Y.H., Field, R.D., and Roswintiarti, O. Trends in atmospheric haze induced  
21 by peat fires in Sumatra Island, Indonesia and El Niño phenomenon from 1973 to  
22 2003. *Geophysical Research Letters* **31**, L04103 (2004).
- 23 9. Logan, J.A. *et al.* Effects of the 2006 El Niño on tropospheric composition as  
24 revealed by data from the Tropospheric Emission Spectrometer (TES). *Geophysical*  
25 *Research Letters* **35**, L03816 (2008).
- 26 10. Rinsland, C.P. *et al.* Tropospheric emission spectrometer (TES) and atmospheric  
27 chemistry experiment (ACE) measurements of tropospheric chemistry in tropical  
28 southeast Asia during a moderate El Niño in 2006. *Journal of Quantitative*  
29 *Spectroscopy & Radiative Transfer* **109**, 1931-1942 (2008).
- 30 11. Li, W.H. *et al.* Future precipitation changes and their implications for tropical  
31 peatlands. *Geophysical Research Letters* **34**, L01403 (2007).
- 32 12. Fargione, J., Hill, J., Tilman, D., Polasky, S., and Hawthorne, P. Land clearing and  
33 the biofuel carbon debt. *Science* **319**, 1235-1238 (2008).
- 34 13. Hansen, M.C. *et al.* Humid tropical forest clearing from 2000 to 2005 quantified by  
35 using multitemporal and multiresolution remotely sensed data. *Proceedings of the*  
36 *National Academy of Sciences of the United States of America* **105**, 9439-9444

- 1 (2008).
- 2 14. van der Werf, G.R., J.T. Randerson, L. Giglio, N. Gobron, and A.J. Dolman.  
3 Climate controls on the variability of fires in the tropics and subtropics. *Global*  
4 *Biogeochemical Cycles* **22**, GB3028, (2008).
- 5 15. Bowen, M.R., Bompard, J.M., Anderson, I.P., Guizol, P., and Gouyon, A.  
6 Anthropogenic Fires in Indonesia: A View from Sumatra. In Eaton, P., Radojevic,  
7 M., and (eds) (eds.) *Forest Fires and Regional Haze in Southeast Asia*. Nova  
8 Science Publishers, Huntington, NY (2001).
- 9 16. Heil, A. and Goldammer, J.G. Smoke-haze pollution: a review of the 1997 episode  
10 in Southeast Asia. *Regional Environmental Change* **2**, 24-37 (2001).
- 11 17. Field, R.D., Wang, Y., Roswintiarti, O., and Guswanto. A drought-based predictor  
12 of recent haze events in western Indonesia. *Atmospheric Environment* **38**, 1869-  
13 1878 (2004).
- 14 18. Cochrane, M.A. Fire science for rainforests. *Nature* **421**, 913-919 (2003).
- 15 19. Saji, N.H., Goswami, B.N., Vinayachandran, P.N., and Yamagata, T. A dipole  
16 mode in the tropical Indian Ocean. *Nature* **401**, 360-363 (1999).
- 17 20. Hong, C.C., Lu, M.M., and Kanamitsu, M. Temporal and spatial characteristics of  
18 positive and negative Indian Ocean dipole with and without ENSO. *Journal of*  
19 *Geophysical Research-Atmospheres* **113**, D08107 (2008).
- 20 21. D'Arrigo, R. and Wilson, R. El Niño and Indian Ocean influences on Indonesian  
21 drought: implications for forecasting rainfall and crop productivity. *International*  
22 *Journal of Climatology* **28**, 611-616 (2008).
- 23 22. van Oldenborgh, G.J., Balmaseda, M.A., Ferranti, L., Stockdale, T.N., and  
24 Anderson, D.L.T. Did the ECMWF seasonal forecast model outperform statistical  
25 ENSO forecast models over the last 15 years? *Journal of Climate* **18**, 3240-3249  
26 (2005).
- 27 23. Vecchi, G.A. and Soden, B.J. Global warming and the weakening of the tropical  
28 circulation. *Journal of Climate* **20**, 4316-4340 (2007).
- 29 24. Notaro, M. Statistical identification of global hot spots in soil moisture feedbacks  
30 among IPCC AR4 models. *Journal of Geophysical Research-Atmospheres* **113**,  
31 D09101 (2008).
- 32 25. Carter, C., Finley, W., Fry, J., Jackson, D., and Willis, L. Palm oil markets and  
33 future supply. *European Journal of Lipid Science and Technology* **109**, 307-314  
34 (2007).
- 35 26. Chen, M.Y., Xie, P.P., Janowiak, J.E., and Arkin, P.A. Global land precipitation: a

- 1           50-Yr monthly analysis based on gauge observations. *Journal of Hydrometeorology*  
2           **3**, 249-266 (2002).
- 3   27. Adler, R.F. *et al.* The Version-2 Global Precipitation Climatology Project (GPCP)  
4           monthly precipitation analysis (1979-Present). *Journal of Hydrometeorology* **4**,  
5           1147-1167 (2003).
- 6   28. Usup A., Hashimoto Y., Takahashi H., and Hayasaka H. Combustion and thermal  
7           characteristics of peat fire in tropical peatland in Central Kalimantan, Indonesia.  
8           *Tropics* **14**, 1-19 (2004).
- 9   29. Efron, B. and Tibshirani, R.J. *An Introduction to the Bootstrap*. Chapman and Hall,  
10          Boca Raton, Florida (1993).
- 11   30. The Land Cover Map for South East Asia in the Year 2000. Stibig, H-J, Upik, R.,  
12          Beuchle, R., Hildanus, and Mubareka, S. 2003. European Commission, Joint  
13          Research Centre.

1 **Tables**

		<b>1960-1983 (PRECL)</b>		<b>1984-2006 (GPCP)</b>	
<b>Sumatra (5-month precipitation)</b>	$R^2$	0.67	(0.39, 0.88)	0.85	(0.68, 0.93)
	$\alpha$ (mm)	609	(468, 826)	631	(538, 756)
	$\beta_0$ ( $\text{km}^{-1}\text{mm}^{-1}$ )	6.9	(1.8, 22.2)	9.8	(5.6, 15.7)
	$\beta_1$ ( $\text{km}^{-1}\text{mm}^{-1}$ )	-0.011	(-0.046, -0.002)	-0.015	(-0.026, -0.007)
	$\beta_2$ ( $\text{km}^{-1}\text{mm}^{-1}$ )	0.010	(0.002, 0.046)	0.015	(0.008, 0.029)
<b>Kalimantan (4-month precipitation)</b>	$R^2$	0.13	(0.02, 0.39)	0.78	(0.60, 0.90)
	$\alpha$ (mm)	524	(254, 1893)	672	(616, 822)
	$\beta_0$ ( $\text{km}^{-1}\text{mm}^{-1}$ )	0.8	(0.2, 5.6)	5.1	(2.8, 7.4)
	$\beta_1$ ( $\text{km}^{-1}\text{mm}^{-1}$ )	-0.001	(-0.013, 0.000)	-0.007	(-0.011, -0.003)
	$\beta_2$ ( $\text{km}^{-1}\text{mm}^{-1}$ )	0.001	(0.000, 0.013)	0.007	(0.003, 0.011)

2

3

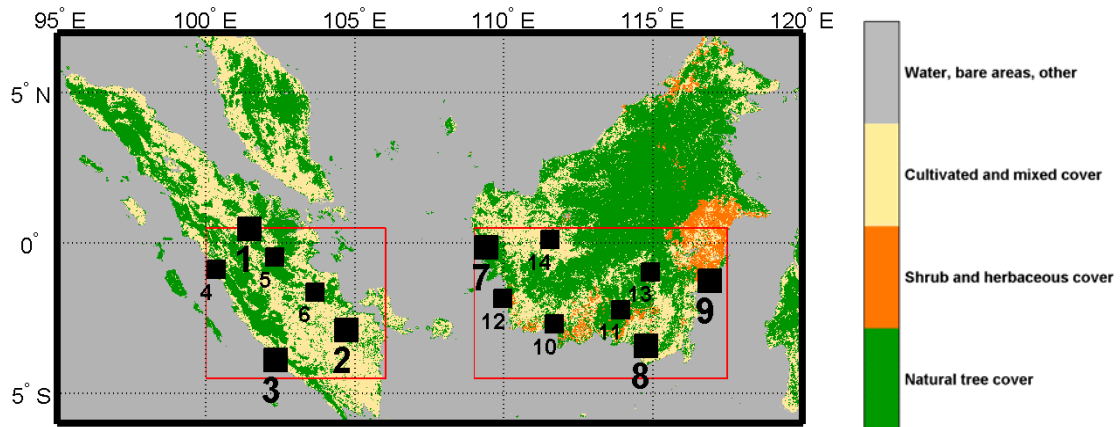
4

5

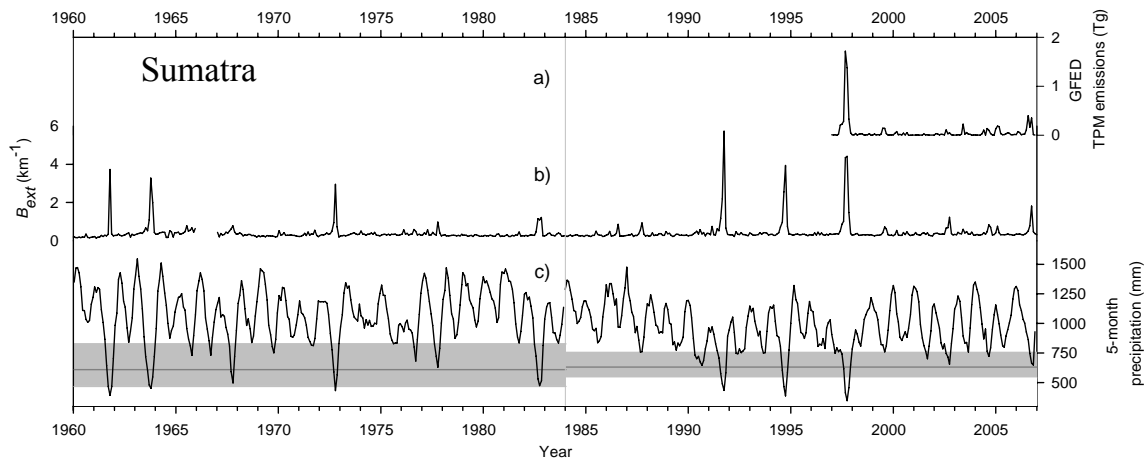
6

**Table 1. Linear piecewise regression estimates, with 95% confidence intervals in parentheses. The parameter  $\alpha$  is the rainfall threshold below which haze events tended to occur. The parameter  $\beta_1$  is the below-threshold slope, or rate at which  $B_{ext}$  changes when precipitation is less than  $\alpha$ . Confidence intervals were estimated using fully-paired bootstrapping with 2000 re-samples.**

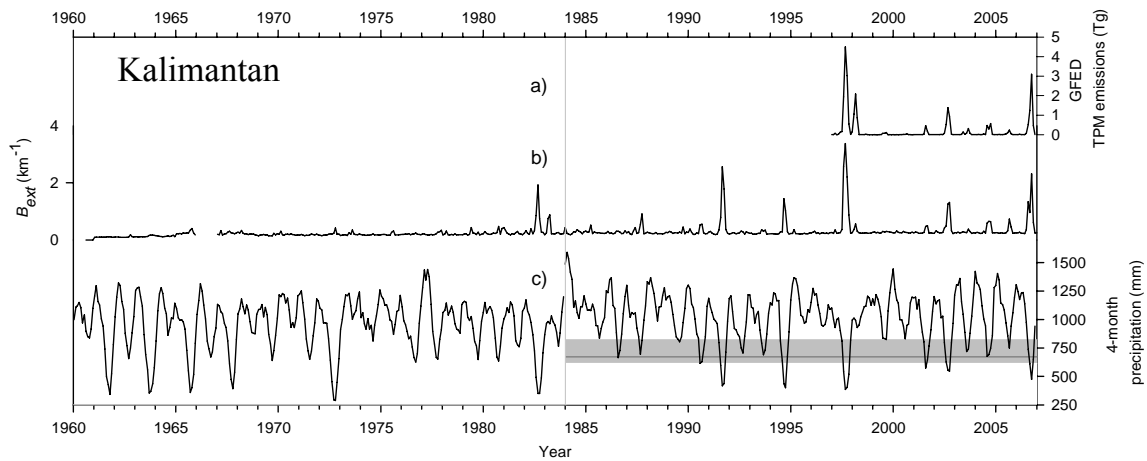
1 **Figures**



2  
3 **Figure 1. Land cover from Global Land Cover 2000<sup>30</sup> and WMO stations used in the analysis, listed**  
4 **in Table S1. Stations 1-3 and 7-9 were used in the long-term analysis. The red box outlines the**  
5 **regions over which TPM emissions, precipitation and population were analysed for Sumatra (0.5N to**  
6 **4.5S, 100E to 106E) and Kalimantan (0.5N to 4.5S, 109E to 117.5E).**  
7



1  
2 **Figure 2. Monthly time-series for Sumatra: a) GFED TPM emissions estimates, b) mean  $B_{ext}$  c) 5-**  
3 **month precipitation from the NCEP Precipitation over Land (PRECL) data<sup>26</sup> for 1960-1983, and**  
4 **Global Precipitation Climatology Project (GPCP)<sup>27</sup>, for 1984-2006. The grey vertical line separates**  
5 **the two analysis periods. The grey horizontal lines in c) show the estimated threshold  $\alpha$  during each**  
6 **period, and the shading shows the 95% confidence interval for  $\alpha$ . Figure S7 shows the  $B_{ext}$  and**  
7 **precipitation data in a scatterplot view.**



1  
2  
3  
4  
5  
6  
7  
8  
9

**Figure 3. Monthly time-series for Kalimantan: a) GFED TPM emissions estimates, b) mean  $B_{ext}$  c) 4-month precipitation from the NCEP Precipitation over Land (PRECL) data<sup>26</sup> for 1960-1983, and Global Precipitation Climatology Project (GPCP)<sup>27</sup>, for 1984-2006. The grey vertical line separates two analysis periods. The grey horizontal line in c) shows the estimated threshold  $\alpha$  during 1984-2006, and the shading shows the 95% confidence interval for  $\alpha$ . No threshold is shown for 1960-1983, due to the poor fit of the model. Figure S8 shows the  $B_{ext}$  and precipitation data in a scatterplot view.**

## Supplementary materials

### 1. Visibility data

Because of its importance in navigation, visibility has been recorded at World Meteorological Organization (WMO)-level stations throughout the world, and used to identify, for example, long-term temporal improvements in air quality over the eastern US associated with reductions in SO<sub>2</sub> emissions<sup>31</sup>, the opposite phenomenon in China's industrial heartland<sup>32,33</sup>, and the impact of dust on visibility during dry periods in North Africa and China<sup>34</sup>.

Visibility observations are made at ground level using landmarks at known distances, and without the aid of optical devices. Distances are measured in increments proportional to their magnitude: in 100m steps between 100 m and 5000 m, in steps of 1km between 6km and 30km, and steps of 5km between 30km and 70km<sup>35</sup>. Visibility observations were obtained from the synoptic meteorological observations in the ds463.0 and ds463.3 archives at the National Center for Atmospheric Research. Over time, there was an increase in the number of hours at which observations were reported. To avoid introducing a diurnal bias over time, we analyzed only the standard 00 and 12 UTC observations, which corresponded to 07:00 and 19:00 local time. Following standard practice, records where the visibility could have been affected by fog or precipitation, and not smoke haze, were excluded<sup>34,36</sup>, based on the values of the present weather codes in the synoptic records.

Extinction coefficient ( $B_{ext}$ ) was calculated from the visibility observations using the Koschmeider relationship<sup>36</sup>:

$$B_{ext} = \frac{K}{V}$$

where  $K$  is the Koschmeider constant and  $V$  is the visibility in km. The Koschmeider constant  $K$  corresponds to the contrast sensitivity threshold of the observer and the inherent contrast between visibility targets and the background sky. We used a value of  $K=1.9$ , following previous studies<sup>31,36</sup>.

Physically,  $B_{ext}$  measures the degree to which visible light is attenuated with distance due to aerosol absorption and scattering, and has units of km<sup>-1</sup>. Instances of 0m-visibility under extreme haze conditions were replaced with 100 m, the next smallest increment at which visibility is recorded. This makes the  $B_{ext}$  used in this analysis conservative during periods of severe haze. For each month, data from the stations across each of Sumatra and Kalimantan were pooled and used to calculate a monthly regional mean. In this way, stations with fewer observations in a given month were not over-represented in the regional signal. In Pontianak, all 00 UTC values from 1960-1964 were missing present weather codes, and so were replaced with the 03 UTC values, when present weather codes were available.

There were six stations in Sumatra and eight stations in Kalimantan, but only three stations in each region had continuous data as far back as 1960 (Figures S3 – S6). The

1 additional stations in Sumatra appear to have been operational in the early 1960s, but  
2 much of the data was missing. Conversely, most of the stations in Kalimantan's main  
3 burning region appear to have been commissioned only in the 1980s. Interestingly, the  
4 availability of this data is due to new airport construction in more remote areas, reflecting  
5 the population growth and development which contributed to the increased severity of the  
6 fire problem. These stations were therefore excluded from the long-term signal, to avoid  
7 artificially inflating the magnitude of the  $B_{ext}$  signal during the 1980s and 1990s.

8  
9 The  $B_{ext}$  signal over Kalimantan does an excellent job of distinguishing the magnitudes  
10 of the 1997, 2002 and 2006 events, when burning was concentrated in the region bounded  
11 by the stations. There was also a significant burning event in early 1998 appearing in the  
12 Kalimantan TPM signal, which occurred exclusively in the province of East Kalimantan<sup>7</sup>  
13 under localized drought conditions<sup>5,17</sup>. This event is captured only weakly by the long-  
14 term  $B_{ext}$  signal for Kalimantan (Figure 3), which reflected the detection of the event in  
15 Balikpapan (966330). The event was also strongly evident at the Muaratewe (965950)  
16 station (Figure S6), which was directly downwind of East Kalimantan, but whose  
17 observations began only in 1984 and were excluded from the long term signal. The  
18 Borneo Mega-fires of early 1983<sup>37</sup> occurred under similar drought conditions, and were  
19 detected most clearly in the Balikpapan records.

20  
21 The additional stations also helped to understand the unprecedented severity of the 1997  
22 event, not only in terms of greenhouse gas emissions<sup>1</sup>, but also with respect to regional  
23 air pollution. For comparison, we considered the  $B_{ext}$  extremes in the five major cities  
24 recognized as having the world's worst air quality in terms of particulate matter<sup>38</sup>.  
25 Indeed, these cities typically had poorer average air quality than the stations in Indonesia,  
26 judging by their mean  $B_{ext}$  values (Table S1). The extreme events in Indonesia, however,  
27 were far worse. Of the five major cities, the highest  $B_{ext}$  was  $3.1 \text{ km}^{-1}$  in Delhi, India,  
28 during December 1998, followed by  $1.9 \text{ km}^{-1}$  in Chongqing, China, in November 2004. In  
29 Sumatra, the highest  $B_{ext}$  was  $16.6 \text{ km}^{-1}$  in Jambi during October of 1997, and in  
30 Kalimantan, the highest  $B_{ext}$  was  $14.1 \text{ km}^{-1}$  in Muaratewe during September of 1997, both  
31 roughly five times greater than in Delhi.

## 32 **2. Sea-surface temperature data**

33 We calculated the Niño 3.4 and Dipole Mode Indices (DMI) using global gridded SST  
34 data<sup>39</sup>. The Niño 3.4 index is defined as the SST anomaly over the 5S-5N and 170W-  
35 120W region. The DMI is defined as the anomaly in temperature difference between the  
36 western equatorial Indian Ocean (50E-70E, 10S-10N) and the southeastern equatorial  
37 Indian Ocean (90E-110E, 10S-0N)<sup>19</sup>.

## 38 **3. Trajectory analysis**

39 We conducted atmospheric trajectory simulations for Pontianak (965810), Banjarmasin  
40 (966850) and Balikpapan (966330) to determine if the absence of haze in the 1960s and  
41 1970s in the Kalimantan  $B_{ext}$  signal could be explained not by the absence of smoke  
42 emissions, but rather by differences in atmospheric flow. Back-trajectories from these  
43 locations were computed using the HYbrid Single-Particle Lagrangian Integrated  
44 Trajectory (HYSPLIT) model<sup>40</sup>, and the wind fields from the NCAR-NCEP Reanalysis

1 <sup>41</sup>. Back trajectories were run from 500m above ground level using a 1-hour time step, for  
2 96 hours in length, for each day in the 1960-2006 period. The eastern region outlined in  
3 Figure 1 was identified as the potential source region over Kalimantan.

4  
5 The absence of haze in the 1960s and 1970s at the Kalimantan stations could not be  
6 explained by different patterns of wind flow. At the Pontianak station in West  
7 Kalimantan, for example, air masses consistently arrived from the southern Kalimantan  
8 burning region in 1972, similar to the haze event of 1997 (Figure S9). Any significant  
9 burning emissions during the 1972 drought would have been detected in Pontianak.  
10 Banjarmasin in South Kalimantan province lies at the eastern edge of the main burning  
11 region, during which the atmospheric flow is from the east. Like Pontianak, there was  
12 little difference in the direction of flow between the 1972 and 1997 events (Figure S10).

13  
14 More quantitatively, we tracked the number of monthly back-trajectory points which fell  
15 within the Kalimantan burning region, as an indicator of the potential source strength  
16 over time. To determine if there was a difference between the droughts during the 1960-  
17 1983 (1961, 1963, 1965, 1967, 1972, 1982) and 1984-2006 (1987, 1991, 1994, 1997,  
18 2002, 2006) periods, we compared the number of trajectory crossings during the dry  
19 months of July-November. In Pontianak, an average of 49.5% ( $\sigma = 13.8$ ) of the trajectory  
20 points fell within the burning regions during the droughts of 1960-1983, compared to  
21 51.9% ( $\sigma = 15.8$ ) during the droughts of 1984-2006, which were not statistically different  
22 using a two-sided t-test ( $p = 0.54$ ). In Banjarmasin, an average of 13.5 ( $\sigma = 10.1$ ) of the  
23 trajectory points fell within the burning regions during 1960-1983, compared to 15.2% ( $\sigma$   
24  $= 11.5$ ) during 1984-2006, also not statistically different using a two-sided t-test ( $p$   
25  $= 0.55$ ). In Banjarmasin, an average of 9.3 ( $\sigma = 9.1$ ) of the trajectory points fell within the  
26 burning regions during 1960-1983, compared to 13.1% ( $\sigma = 11.6$ ) during 1984-2006, also  
27 not statistically different using a two-sided t-test ( $p = 0.17$ ). We note also that the weaker  
28 absolute magnitudes of the  $B_{ext}$  signal in Banjarmasin and Balikpapan (Figure S11)  
29 reflects their location at the upwind extent of Kalimantan's main burning region.

#### 30 **4. Deforestation and peatland drainage**

31 Forest cover estimates for 1950, 1985 and 1997 (Table S2) were used to calculate annual  
32 rates of deforestation  $q$  using

$$33 \quad q = \left( \frac{A_2}{A_1} \right)^{1/(t_2 - t_1)} - 1$$

34 where  $A_2$  and  $A_1$  are the forest cover at  $t_1$  and  $t_2$  <sup>42, 43</sup>. The rapid increase in deforestation  
35 rates for both regions corresponds to a substantial increase in logging, with log  
36 production increasing in the 1970s by a factor of five from 5 000 000 m<sup>3</sup> in the 1960s to  
37 over 25 000 000 m<sup>3</sup> in the 1980s <sup>42</sup>. There was also a significant growth in land  
38 allocated for agricultural and estate crops, with oil palm plantations in particular  
39 exhibiting rapid expansion in the late 1980s <sup>42, 44</sup>.

40  
41 Perhaps the single biggest contributor to Kalimantan's increase in fire sensitivity was the  
42 Mega Rice Project (MRP) in Central Kalimantan. Starting in 1995, an area of almost one  
43 million ha was cleared from peat swamp forest, and over 4400 km of drainage canals

1 were constructed to make the land suitable for rice agriculture. The peat conditions were  
2 unsuitable for rice cultivation, and the sole legacy of the project was one million ha of  
3 drained peatlands no longer resilient to drought, and vulnerable to carbon release from  
4 oxidation<sup>45</sup> and fire. The MRP area was in fact the single biggest contributor to  
5 Indonesia's unprecedented emissions in 1997 from biomass burning<sup>5</sup>, which constituted  
6 to up to 40% of annual global fossil fuel emissions at that time<sup>1</sup>.

## 7 **5. Population growth and transmigration**

8 Transmigration had occurred for over a century in Indonesia<sup>46</sup>, but its importance  
9 increased in the 1960s under the Suharto government, with financial aid from  
10 international donors<sup>47</sup>. Sumatra was the main target region of transmigration in earlier  
11 stages, due to already established populations and easier access from Java<sup>46</sup>, which is  
12 separated by only 25 km of sea at its nearest point. From 1951-1969, 83% of  
13 transmigrants were settled in Sumatra, compared to 11% in Kalimantan<sup>48</sup>. From 1969 to  
14 1974, Sumatra continued to be the primary destination (58%), although the proportion  
15 destined for Kalimantan had increased to 15%, with a greater emphasis on Sulawesi  
16 (26%). At the end of the third phase of planned transmigration in 1984, 62% of families  
17 settled in Sumatra, compared to 19% in Kalimantan. The first World Bank-sponsored  
18 transmigration phase which explicitly included Kalimantan was initiated only in 1983<sup>46</sup>.  
19 During the 1984/5 to 1988/9 phase, Kalimantan became the planned primary target  
20 (42%), with Sumatra a secondary target (27%)<sup>49</sup>, although it was not clear whether this  
21 reversal had been achieved<sup>50</sup>.

22  
23 At the same time Kalimantan was included as a target region in the 1980s, the focus of  
24 the transmigration program shifted from small-scale subsistence farming to large-scale  
25 industrial agriculture such as rubber, oil palm, and forest plantations for fuel, pulp and  
26 plywood<sup>44,46 51</sup>. This shift can result in an increase in per capita land use, for example  
27 from 2-5 ha/family for agriculture compared to 20 ha/family for silviculture, as reported  
28 for Thailand<sup>52</sup>, amplifying the impact in Kalimantan of newly arriving populations.  
29

1 **Supplementary references**

- 2 31. Schichtel, B.A., Husar, R.B., Falke, S.R., and Wilson, W.E. Haze Trends Over the  
3 United States, 1980-1995. *Atmospheric Environment* **35**, 5205-5210 (2001).
- 4 32. Qian, Y. and Giorgi, F. Regional Climatic Effects of Anthropogenic Aerosols? The  
5 Case of Southwestern China. *Geophysical Research Letters* **27**, 3521-3524 (2000).
- 6 33. Che, H.Z., Zhang, X.Y., Li, Y., Zhou, Z.J., and Qu, J.J. Horizontal visibility trends  
7 in China 1981-2005. *Geophysical Research Letters* **34**, L24706 (2007).
- 8 34. Mahowald, N.M., Ballantine, J.A., Feddema, J., and Ramankutty, N. Global trends  
9 in visibility: implications for dust sources. *Atmospheric Chemistry and Physics* **7**,  
10 3309-3339 (2007).
- 11 35. World Meteorological Organization. *Guide to Meteorological Instruments and*  
12 *Methods of Observation*. World Meteorological Organization, Geneva, Switzerland  
13 (1996).
- 14 36. Husar, R.B., Husar, J.D., and Martin, L. Distribution of Continental Surface  
15 Aerosol Extinction Based on Visual Range Data. *Atmospheric Environment* **34**,  
16 5067-5078 (2000).
- 17 37. Malingreau, J.P., Stephens, G., and Fellows, L. Remote-Sensing of Forest-Fires -  
18 Kalimantan and North-Borneo in 1982-83. *Ambio* **14**, 314-321 (1985).
- 19 38. 2007 World Development Indicators. World Bank. 2007.
- 20 39. Smith, T.M. and Reynolds, R.W. Extended Reconstruction of Global Sea Surface  
21 Temperatures Based on Coads Data (1854-1997). *Journal of Climate* **16**, 1495-1510  
22 (2003).
- 23 40. Draxler, R.R. and Hess, G.D. An Overview of the Hysplit\_4 Modelling System for  
24 Trajectories, Dispersion and Deposition. *Australian Meteorological Magazine* **47**,  
25 295-308 (1998).
- 26 41. Kalnay, E. *et al.* The NCEP/NCAR 40-Year Reanalysis Project. *Bulletin of the*  
27 *American Meteorological Society* **77**, 437-471 (1996).
- 28 42. FWI/GFW. The State of the Forest: Indonesia. Forest Watch Indonesia/Global  
29 Forest Watch. 2002. Bogor, Indonesia, Bogor, Indonesia: Forest Watch Indonesia,  
30 and Washington DC: Global Forest Watch.
- 31 43. Puyravaud, J.P. Standardizing the calculation of the annual rate of deforestation.  
32 *Forest Ecology and Management* **177**, 593-596 (2003).
- 33 44. Gellert, P.K. A brief history and analysis of Indonesia's forest fire crisis. *Indonesia*  
34 **65**, 63-85 (1998).

- 1 45. Hooijer, A., M. Silvius, H. Wösten, and S. Page. PEAT-CO2, Assessment of CO2  
2 emissions from drained peatlands in SE Asia. 2006. Delft Hydraulics.
- 3 46. Fearnside, P.M. Transmigration in Indonesia: lessons from its environmental and  
4 social impacts. *Environmental Management* **21**, 553-570 (1997).
- 5 47. World Bank. Indonesia transmigration program: A review of five bank supported  
6 projects. 1994.
- 7 48. Suratman and P. Guinness. The Changing Focus of Transmigration. *Bulletin of*  
8 *Indonesia Economic Studies* **13**, 78-101 (1977).
- 9 49. Hardjono, J. Transmigration: looking to the future. *Bulletin of Indonesia Economic*  
10 *Studies* **22**, 28-53 (1986).
- 11 50. Leinbach, T.R. The Transmigration Programme in Indonesian National  
12 Development Strategy: Current Status and Future Requirements. *Habitat*  
13 *International* **13**, 81-93 (1989).
- 14 51. Barber, C. V. and Schweithelm, J. Trial by fire: Forest fires and forestry policy in  
15 Indonesia's era of crisis and reform. 2000. Washington, DC, World Resources  
16 Institute.
- 17 52. Lohmann, L. Commercial tree plantations in Thailand: Deforestation by any other  
18 name. *The Ecologist* **20**, 9-17. 1990.
- 19 53. Klein Goldewijk, K. Estimating global land use change over the past 300 years: The  
20 HYDE Database. *Global Biogeochemical Cycles* **15**, 417-433 (2001).

1 **Supplementary tables**

Map ID	WMO ID	Station Name	Elevation (m)	Latitude	Longitude	Mean $B_{ext}$ ( $\text{km}^{-1}$ )	Max $B_{ext}$ ( $\text{km}^{-1}$ )
1	961090	PAKANBARU	31	0.5	101.5	0.5	7.6
2	962210	PALEMBANG	10	-2.9	104.7	0.5	9.5
3	962530	BENGKULU	16	-3.9	102.3	0.3	2.7
4	961630	PADANG	30	-0.9	100.4	0.2	2.5
5	961710	RENGAT	46	-0.5	102.3	0.6	13.1
6	961950	JAMBI	25	-1.6	103.7	0.6	16.6
7	965810	PONTIANAK	3	-0.2	109.4	0.4	5.9
8	966850	BANJARMASIN	20	-3.4	114.8	0.3	3.9
9	966330	BALIKPAPAN	30	-1.3	116.9	0.2	2.4
10	966450	PANGKALANBUN	25	-2.7	111.7	0.5	11.6
11	966550	PALANGKARAYA	27	-2.2	113.9	0.7	11.6
12	966150	KETAPANG	9	-1.9	110.0	0.4	8.3
13	965950	MUARATEWE	60	-1.0	114.9	0.6	14.1
14	965590	SINTANG	30	0.1	111.5	0.5	13.5
	623660	CAIRO, EGYPT	740	30.1	31.4	0.4	1.6
	421820	DELHI, INDIA	2160	28.6	77.2	0.9	3.1
	428090	CALCUTTA, INDIA	60	22.7	88.5	0.8	1.4
	545270	TIANJIN, CHINA	50	39.1	117.2	0.2	0.8
	575150	CHONG-QING, CHINA	3510	29.5	106.5	0.6	1.9

2 **Table S1. Descriptors and summary  $B_{ext}$  statistics for 1973-2006 for Indonesian stations 1 – 14**  
3 **plotted in Figure 1. The last five stations are those for cities identified as having the world’s worst air**  
4 **quality, in terms of  $\text{PM}_{10}$  <sup>38</sup>.**

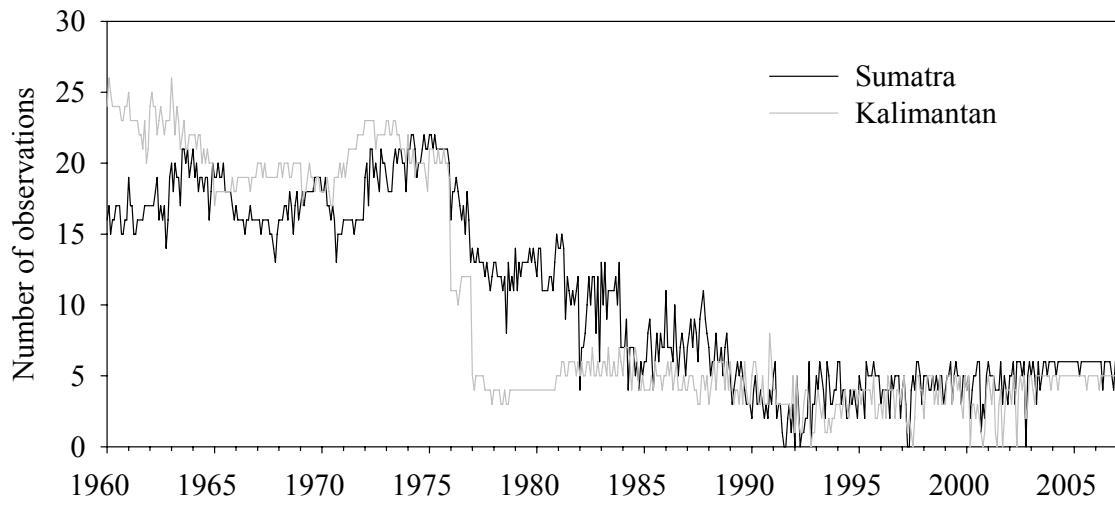
5

1

Year	Indonesia		Sumatra		Kalimantan	
	GOI-WB	GFW-WRI	GOI-WB	GFW-WRI	GOI-WB	GFW-WRI
1950	162 290 000	162 290 000	37 370 000	37 370 000	51 400 000	51 400 000
1985	119 700 500	117 191 550	22 323 500	22 938 825	39 986 000	39 644 025
1997	100 000 000	95 628 800	16 632 143	16 430 300	31 512 208	29 637 475

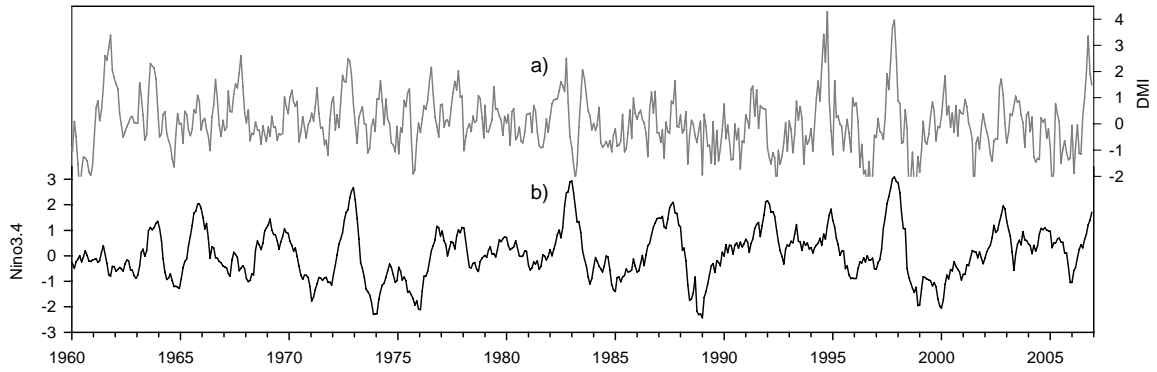
2 **Table S2. Forest cover estimates (in hectares) for Indonesia, Sumatra and Kalimantan, from the**  
3 **Government of Indonesia and World Bank (GOI-WB), and the Global Forest Watch of the World**  
4 **Resources Institute (GFW-WRI) <sup>42</sup>.**

1 **Figures**



2  
3  
4

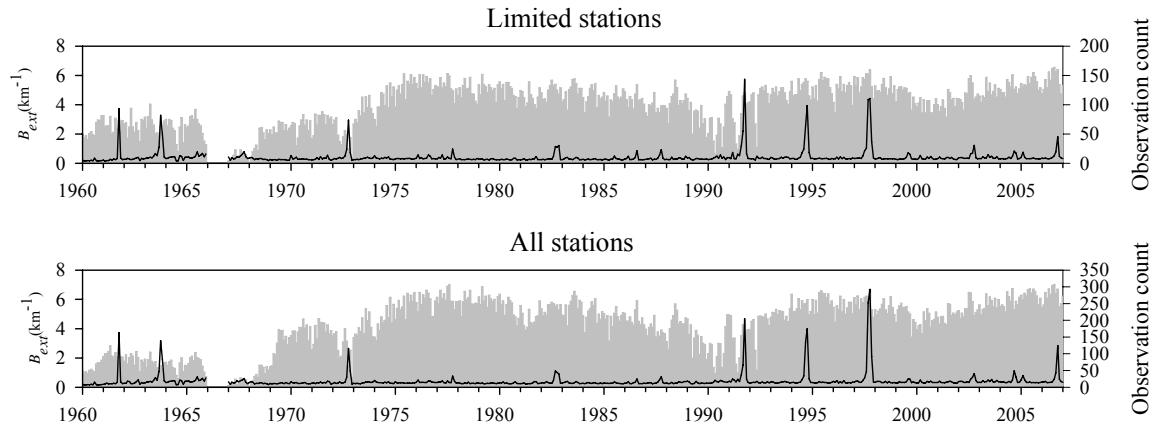
**Figure S1. Monthly PRECL precipitation observation counts for Kalimantan and Sumatra.**



1  
2  
3  
4  
5

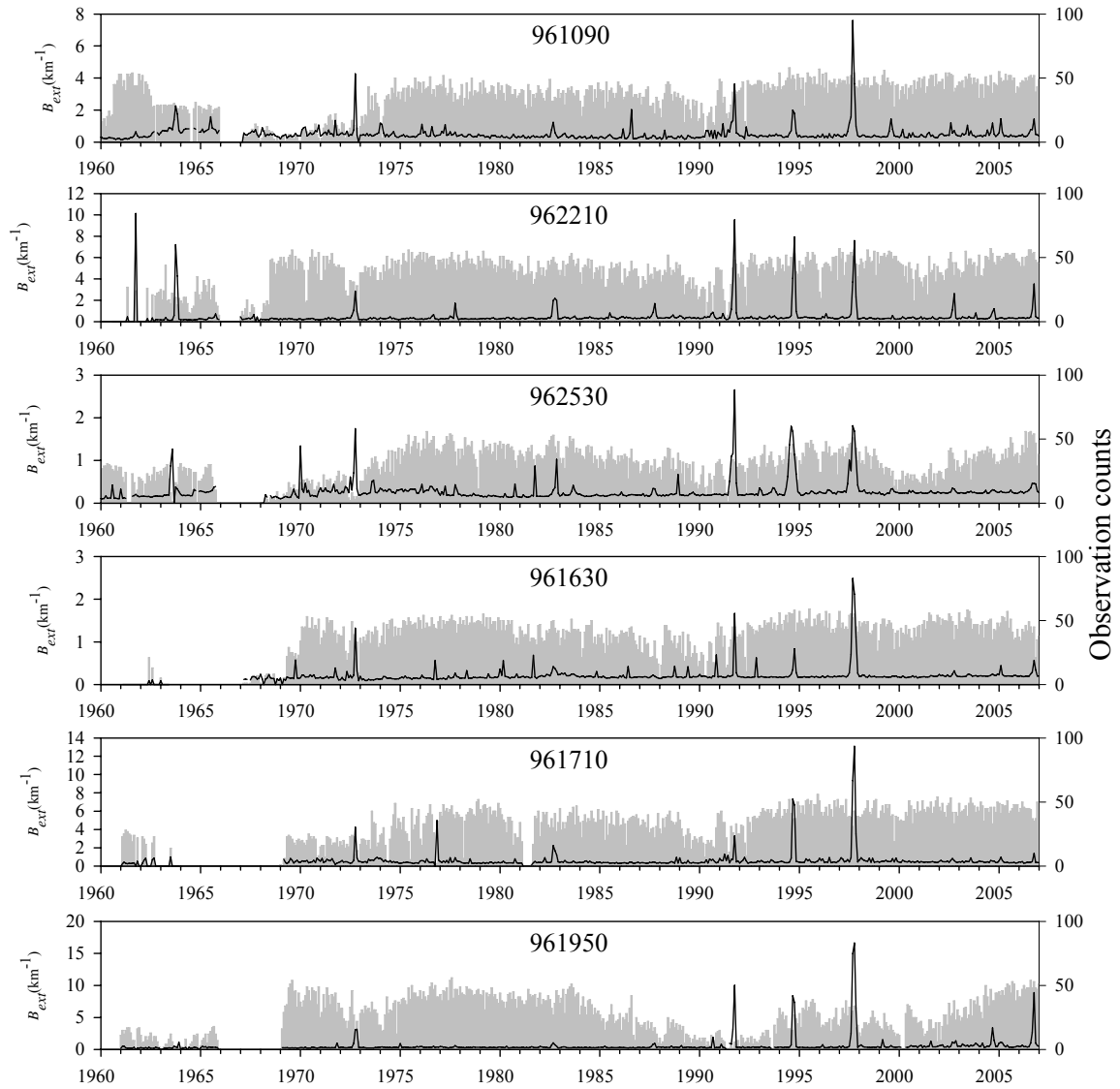
**Figure S2. Monthly sea surface temperature anomalies calculated from global gridded sea-surface temperature analysis<sup>39</sup>: a) Dipole Mode Index<sup>19</sup> b) Niño3.4 index. Both indices have been centralized and standardized to 0-mean and 1- $\sigma$  standard error.**

1



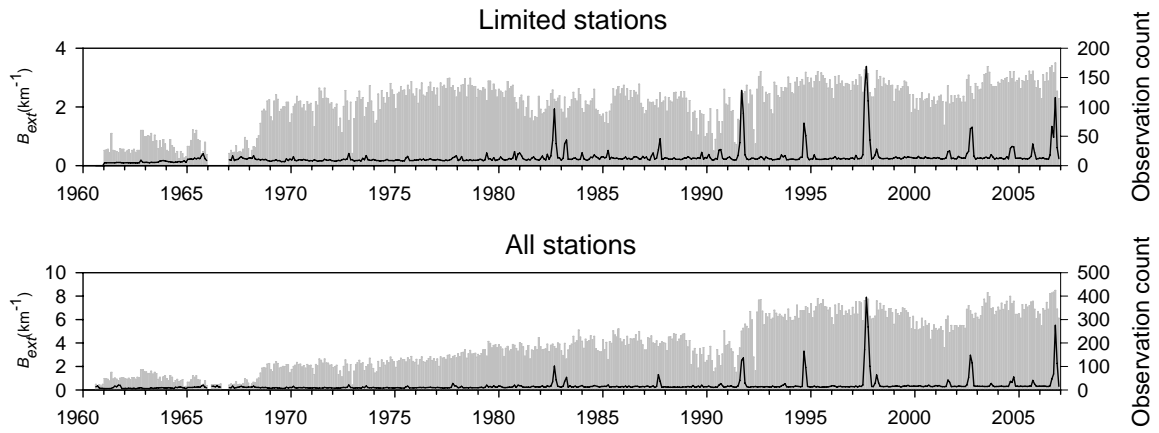
2  
3  
4

**Figure S3. Regional  $B_{ext}$  for Sumatra using a) the long-term stations only b) all available stations. The solid black line shows the  $B_{ext}$  and the vertical grey bars show the number of observations.**

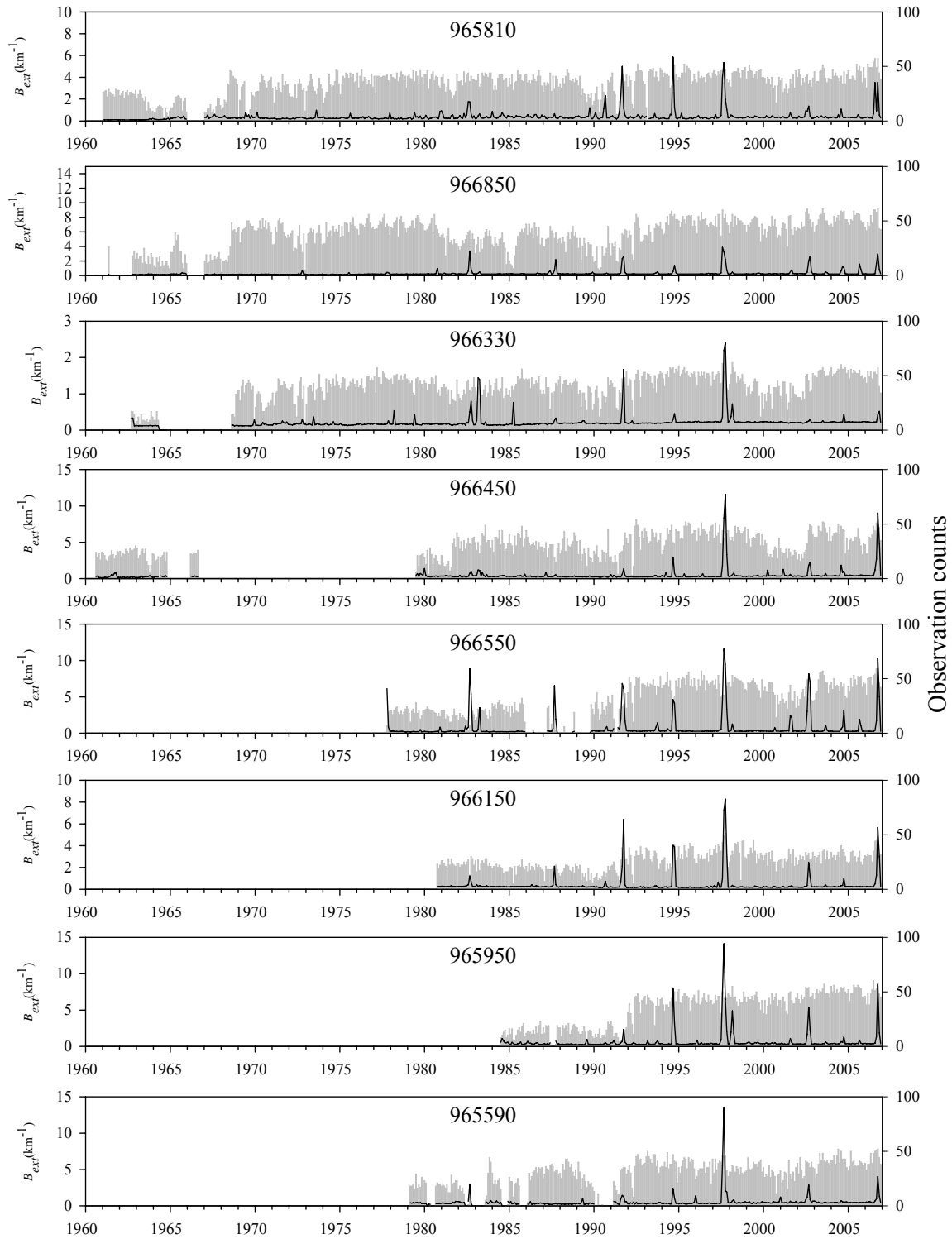


1  
2  
3  
4  
5  
6

Figure S4.  $B_{ext}$  for individual stations in Sumatra. The solid black line shows the  $B_{ext}$  and the vertical grey bars show the number of observations.

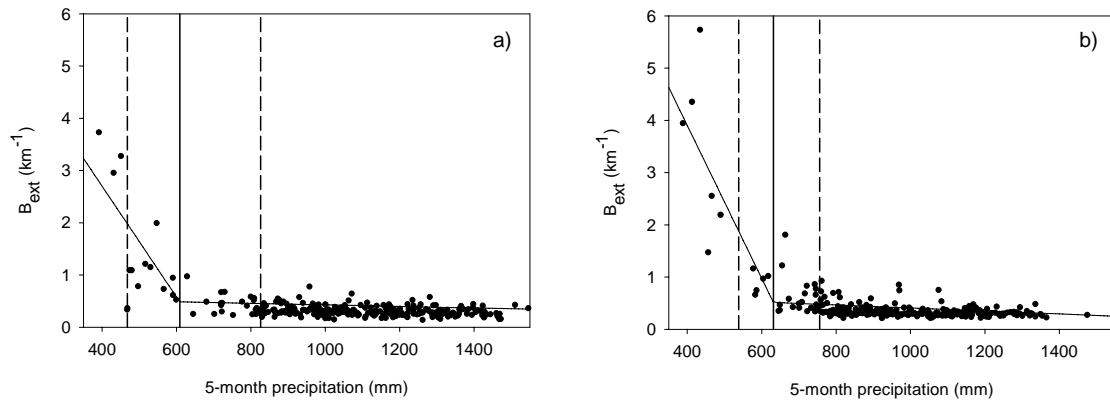


1  
2 **Figure S5. Regional  $B_{ext}$  for Kalimantan using a) the long-term stations only b) all available stations.**  
3 **The solid black line shows the  $B_{ext}$  and the vertical grey bars show the number of observations.**



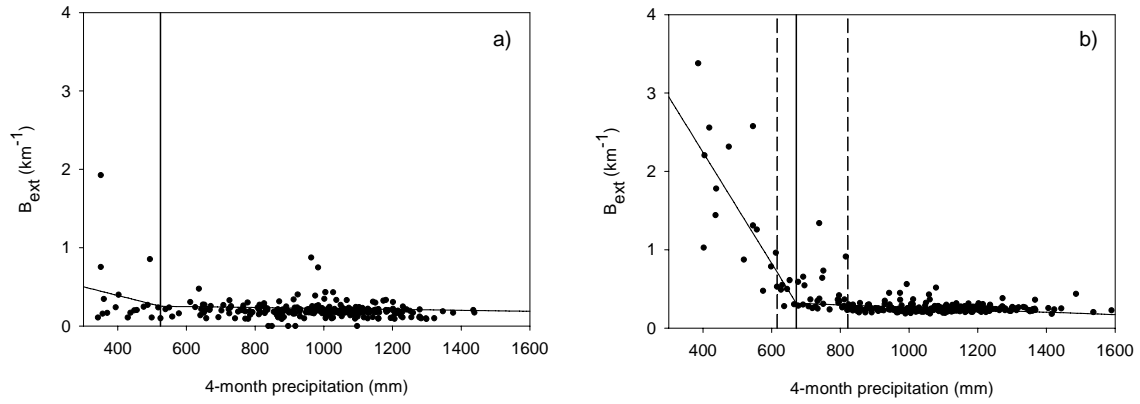
1  
2  
3  
4  
5

Figure S6.  $B_{ext}$  for individual stations in Kalimantan. The solid black line shows the  $B_{ext}$  and the vertical grey bars show the number of observations.



1  
 2 **Figure S7. Sumatra piecewise regression fits for a) 1960-1983 b) 1984-2006. The solid vertical lines**  
 3 **show the threshold estimate and the dashed lines show 95% confidence intervals. This is the same**  
 4 **data as in Figure 2, but in a scatterplot view.**

1



2

3

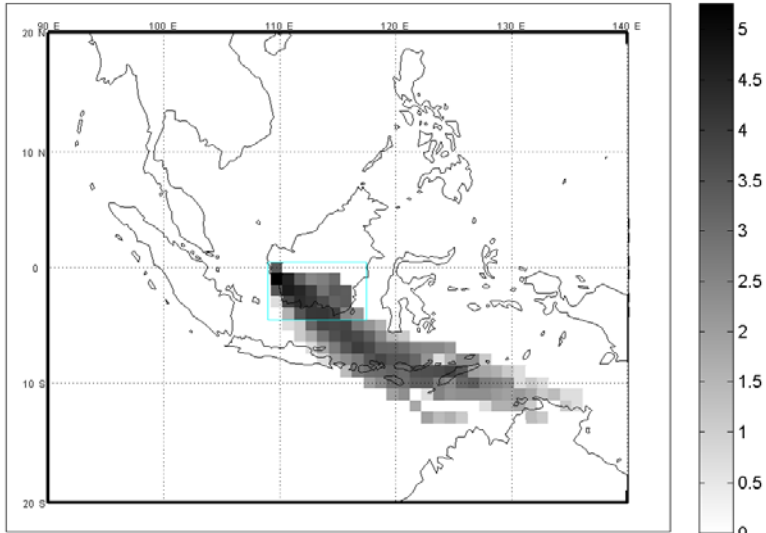
4

5

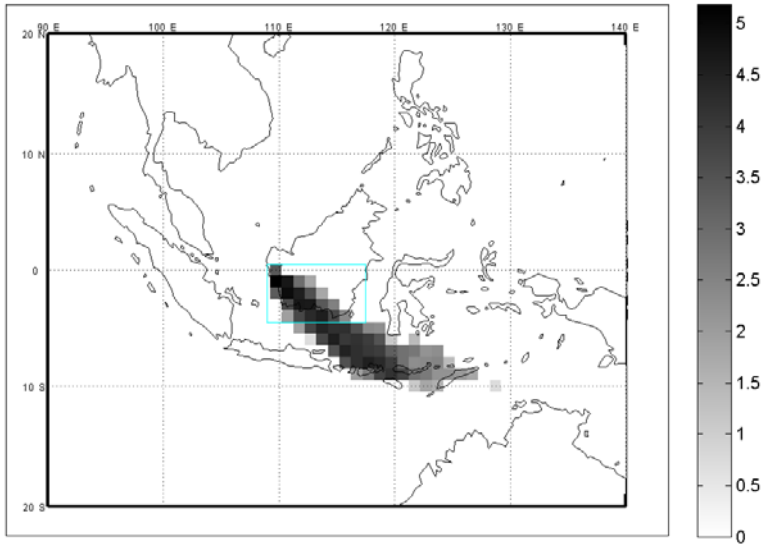
6

**Figure S8. Kalimantan piecewise regression fits for a) 1960-1983 b) 1984-2006. The solid vertical lines shows the threshold estimate and the dashed lines show 95% confidence intervals. This is the same data as in Figure 3, but in a scatterplot view. The threshold estimate for 1960-1983 was not well-constrained and confidence intervals are not shown.**

1  
2

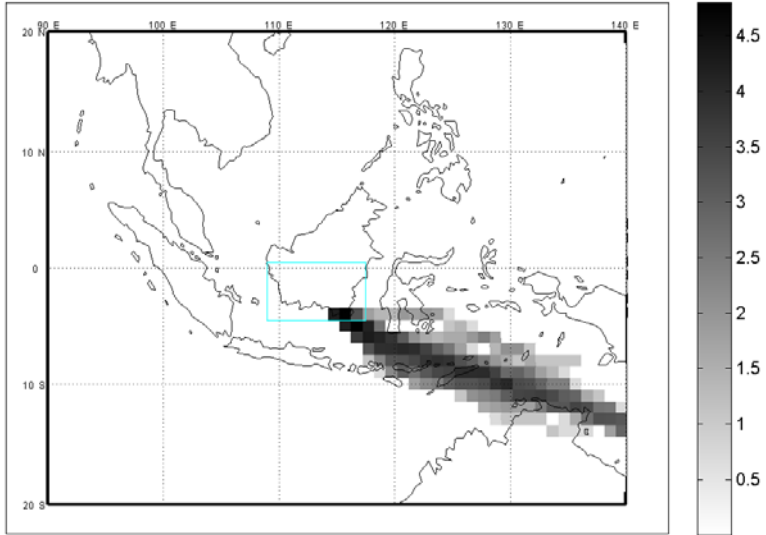


3

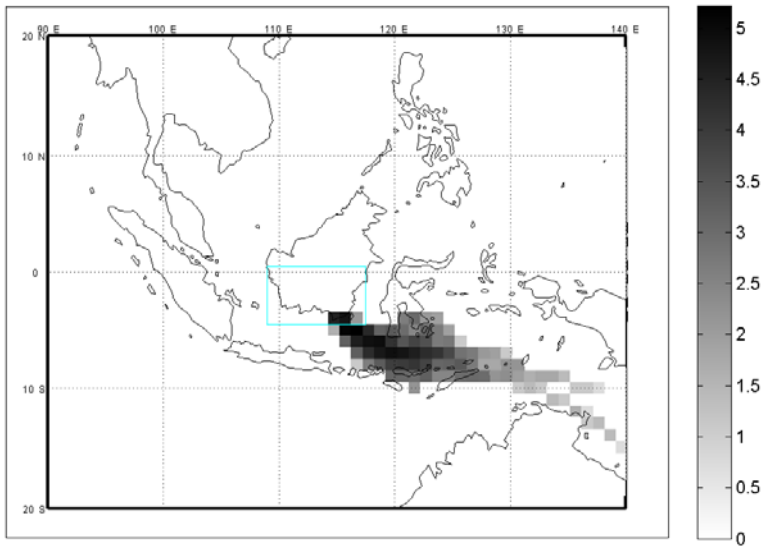


4

5 **Figure S9. Pontianak back trajectory density count maps for September of 1972 (top) and 1997**  
6 **(bottom). The shaded areas show the density of trajectory points, on a logarithmic scale, where**  
7 **darker areas represent areas more frequently crossed by air masses arriving at Pontianak. The blue**  
8 **box outlines the same Kalimantan analysis region in Figure 1.**



1



2

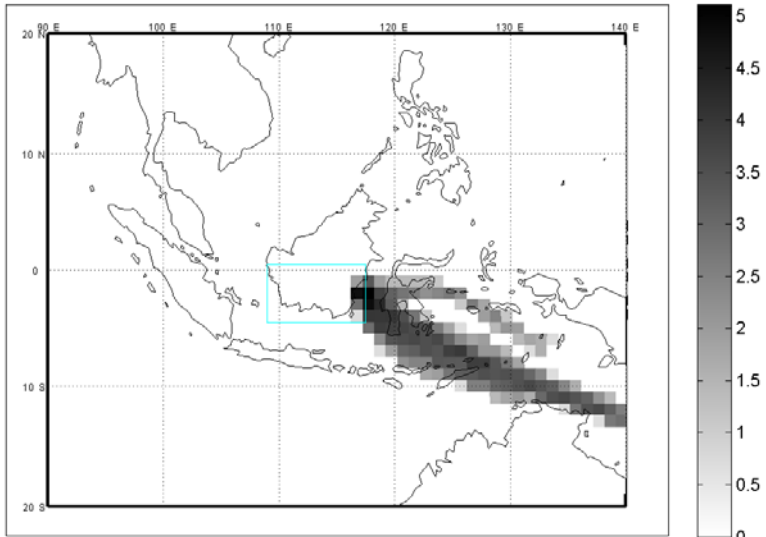
3

4

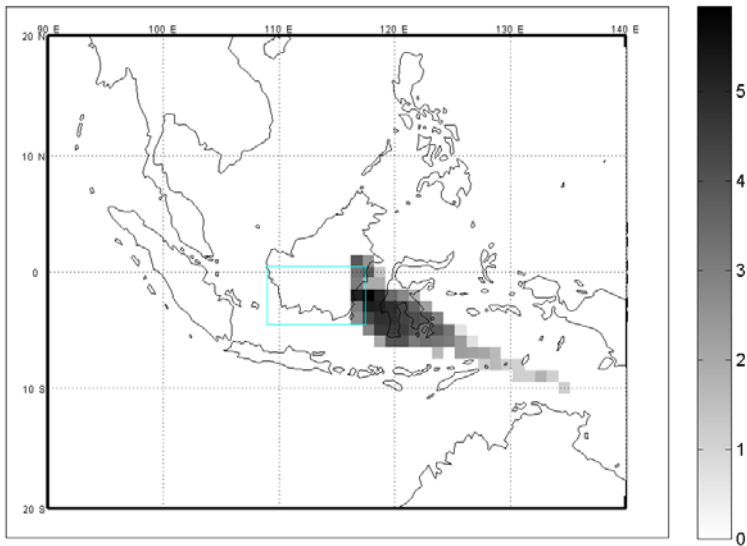
5

6

**Figure S10. Banjarmasin back trajectory density count maps for September of 1972 (top) and 1997 (bottom). The shaded areas show the density of trajectory points, on a logarithmic scale, where darker areas represent areas more frequently crossed by air masses arriving at Pontianak. The blue area outlines the same Kalimantan analysis region in Figure 1.**

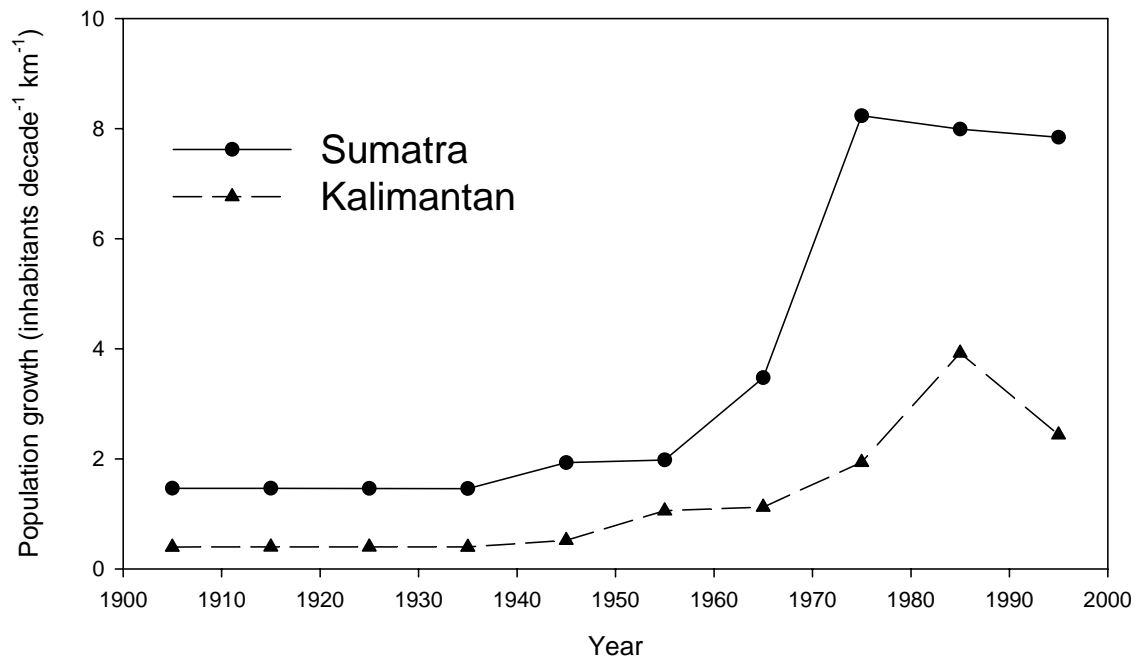


1



2  
3  
4  
5  
6  
7  
8

**Figure S11. Balikpapan back trajectory density count maps for September of 1972 (top) and 1997 (bottom). The shaded areas show the density of trajectory points, on a logarithmic scale, where darker areas represent areas more frequently crossed by air masses arriving at Pontianak. The blue area outlines the same Kalimantan analysis region in Figure 1.**



1  
2  
3  
4

Figure S12. Population growth in southern Sumatra and southern Kalimantan from HYDE database